

PRIMAL: Pathfinding via Reinforcement and Imitation Multi-Agent Learning

Guillaume Sartoretti¹, Justin Kerr¹, Yunfei Shi¹, Glenn Wagner²,
T. K. Satish Kumar³, Sven Koenig³, and Howie Choset¹

Abstract—Multi-agent path finding (MAPF) is an essential component of many large-scale, real-world robot deployments, from aerial swarms to warehouse automation to collaborative search-and-rescue. However, despite the community’s continued efforts, most state-of-the-art MAPF algorithms still rely on centralized planning, and scale poorly past a few hundred agents. Such planning approaches are maladapted to real-world deployment, where noise and uncertainty often require paths to be recomputed or adapted online, which is impossible when planning times are in seconds to minutes. In this work, we present PRIMAL, a novel framework for MAPF that combines reinforcement and imitation learning to teach fully-decentralized policies, where agents reactively plan paths online in a partially-observable world while exhibiting implicit coordination. Our framework extends our previous works on distributed learning of collaborative policies by introducing demonstrations of an expert MAPF algorithm during training, as well as careful reward shaping and environment sampling. Once learned, the resulting policy can be copied onto any number of agents, and naturally scales to different team sizes and world dimensions. We present results on randomized worlds with up to 1024 agents and compare success rates against state-of-the-art MAPF algorithms. Finally, we show experimental results of the learned policies in a hybrid simulation of a factory mock-up, involving both real-world and simulated robots.

I. INTRODUCTION

Given the rapid development of affordable robots with embedded sensing and computation capabilities, manufacturing applications will soon involve the deployment of hundreds, if not thousands, of robots [1], [2]. To support these applications, significant research effort has been devoted to multi-agent path finding (MAPF) [3], [4], [5], [6], to support deployments in distribution centers, potential use for airplane taxiing and multi-agent search and rescue [7], [8], [9]. However, as the number of agents in the system grows, so does the complexity of coordinating them. Current state-of-the-art optimal planners can plan for up to several hundreds of agents, and the community is now settling for bounded suboptimal planners as a potential solution for even larger multi-agent systems [10], [3]. Another common approach is to rely on reactive planners, which do not plan joint paths for all agents before execution, but rather correct

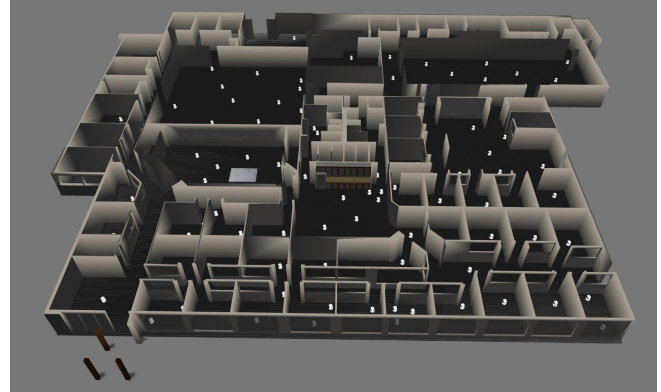


Fig. 1. Example problem where 100 simulated robots (white dots) must compute individual, collision-free paths in a large factory-like environment.

individual paths online to avoid collisions [11], [5]. However, such planners often prove inefficient in cluttered factory environments (such as Fig. 1), where they can result in dead- and livelocks [5].

We propose to approach the MAPF problem from the standpoint of distributed reinforcement learning (RL) [12] to teach each agent to plan its path online. Extending our previous works on distributed RL for multiple agents in shared environments [13], [14], we present PRIMAL, a hybrid approach encompassing both direct RL and imitation learning (IL) from an expert centralized MAPF algorithm. In our approach, agents learn to take into account the consequences of their position on other agents, in order to favor movements that will benefit the whole team and not only themselves. That is, by simultaneously learning to plan efficient single-agent paths (mostly via RL), and to imitate a centralized expert (IL), agents ultimately learn a decentralized policy where they still exhibit implicit coordination during path planning. Since multiple agents learn a common, single-agent policy, the final learned policy can be copied onto any number of agents. Additionally, we consider the case where agents evolve in a partially-observable world, where they can only observe the world in a limited field of view (FOV) around themselves. We present the results of an extensive set of simulation experiments, and show that the final, trained policies naturally scale to various team sizes and world sizes. We further highlight cases where PRIMAL outperforms other state-of-the-art MAPF planners and cases where it struggles. We also present results where the trained policy is deployed on real-world and simulated robots in a hybrid simulation of an indoor factory mockup.

The paper is structured as follows: In Section II, we briefly

G. Sartoretti, H. Choset, J. Kerr, Y. Shi are with the Robotics Institute at Carnegie Mellon University, Pittsburgh, PA 15213, USA. {gsartore, choset}@cs.cmu.edu, {jgkerr, yunfeis}@andrew.cmu.edu.
G. Wagner is with the Commonwealth Scientific and Industrial Research Organisation (CSIRO), Pullenvale QLD 4069, Australia, glenn.s.wagner@gmail.com.
T. K. S. Kumar and S. Koenig are with the Computer Department at the University of Southern California, Los Angeles, CA 90089, USA. tkskwork@gmail.com, skoenig@usc.edu.

summarize the state-of-the-art in multi-agent path finding and reinforcement learning. We then detail how the MAPF problem is cast into the RL framework in Section III, and how learning is carried out in Section IV. Section V presents our results, and Section VI concluding remarks.

II. PRIOR WORKS

A. Multi-Agent Path Finding (MAPF)

MAPF approaches can be broadly separated into three categories: coupled, decoupled, and dynamically-coupled approaches. Coupled approaches (e.g., standard A^*), which treat the multi-agent system as a single, very high dimensional agent, greatly suffer from the exponential growth in planning complexity. Hence we focus on decoupled and dynamically-coupled, state-of-the-art planners for large MAPF problems.

Decoupled approaches compute individual paths for each robot, and then adjust these paths to avoid collisions. Since planning individual paths, as well as adjusting for collisions, can be performed in low-dimensional search spaces, decoupled approaches can rapidly find paths for large multi-agent systems [5], [15]. Velocity planners fix the individual path that will be followed by each robot, then find a velocity profile along those paths that avoids collisions [6], [11]. In particular, ORCA [5] adapts the agents' velocity magnitudes and directions online to avoid collisions, on top of individually-planned single-agent paths, and recent works have focused on such obstacle avoidance approach using reinforcement learning [11]. Priority planners assign a priority to each robot, and plan individual paths in decreasing order of priority, each time treating higher priority robots as moving obstacles [16], [17]. The main drawback of decoupled algorithms is that the low-dimensional search spaces used only represent a small portion of the joint configuration space, meaning that these algorithms cannot always be *complete* (i.e., find a path for all solvable problems) [18].

Several recent approaches lie between coupled and decoupled approaches: they allow for more rich robot-robot behaviors than can be achieved with decoupled planners, while avoiding planning in the joint configuration space. A common approach followed by dynamically coupled algorithms is to grow the search space as necessary during planning [3], [19]. Conflict-Based Search (CBS) [4], [19] plans for individual robots and constructs a set of constraints to find optimal/near-optimal solutions without exploring higher-dimensional spaces. Extending standard A^* to MAPF, M^* and its variants [3] first plan paths for individual robots, and then play these individual plans forward through time searching for collisions. The configuration space is only locally expanded around collisions between single-agent plans, where joint planning is performed through (usually limited) backtracking to solve the collision and resume single-agent plans. In particular, OD-recursive- M^* (ODrM*) [20] can further reduce the dimension of the set of agents for which joint planning is necessary, by breaking it down into independent collision sets, combined with Operator Decomposition (OD) [21] to keep the branching factor small during search.

B. Multi-Agent Reinforcement Learning (MARL)

The first and most important problem encountered when transitioning from single- to multi-agent learning is the curse of dimensionality: most joint approaches fail as the state-action spaces explode combinatorially, requiring impractical amounts of training data to converge [22]. In this context, many recent works have focused on decentralized policy learning [23], [24], [25], [26], [27], where agents each learn their own policy, which should encompass a measure of agent cooperation, at least during training. One such approach is to train agents to predict other agents' actions [24], [25], which generally scales poorly as the team size increases. In most cases, some form of centralized learning is involved, where the sum of experience of all agents can be used towards training a common aspect of the problem (e.g., network output or value/advantage calculation) [23], [25], [26]. When centrally learning a network output, parameter sharing has been used faster and more stable training by sharing the weights of some of the layers of the neural net [23]. In actor-critic approaches, for example, the critic output of the network is often trained centrally with parameter sharing, since it applies to all agents in the system, and has been used to train cooperation between agents [23], [25]. Centralized learning can also help when dealing with partially-observable systems, by aggregating all the agents' observations into a single learning process [23], [25], [26].

Second, many existing approaches rely on explicit communication among agents, to share observations or selected actions during training and sometimes policy execution [24], [25], [26]. In our previous works [13], [14], we focused on extending the state-of-the-art asynchronous advantage actor-critic (A3C) algorithm to enable multiple agents to learn a common, homogeneous policy in shared environments without the need for any explicit agent communications. That is, agents had access to the full state of the system (fully-observable world), and treated each other as moving obstacles. There, stabilizing learning was key: the learning gradients obtained by agents experiencing the same episode in the same environment were often very correlated and destabilized the learning process. To prevent this, we relied on experience replay [28], and carefully randomized episode initialization. However, we did not train agents to exhibit any form of coordination. That is, in our previous extension of A3C, agents **collaborate** (i.e., work towards a common goal) but do not explicitly **cooperate** (i.e., take actions that are beneficial to the whole group and not only themselves). In this work, we propose relying on imitation learning of an expert centralized planner (in this work, ODrM*) to train agents to exhibit coordination, without the need for explicit communications, in a partially-observable world. We also propose a carefully crafted reward structure, as well as a way to sample the challenges (episodes) that are presented to the agents during training. The resulting, trained policy is enacted by each agent based on locally gathered information while still allowing agents to exhibit cooperative behaviors.

III. POLICY REPRESENTATION

In this section, we present how the MAPF problem is cast into the RL framework. We detail the observation and action spaces of each agent, the reward structure used and the neural network that represents the policy to be learned.

A. Observation Space

We consider a partially observable discrete grid world, where agents can only observe the state of the world in limited field of view (FOV) centered around themselves (10×10 FOV in practice). We believe that considering a partially observable world is a realistic and crucial assumption, especially towards real-world robot deployments. Additionally, assuming a fixed FOV can allow the policy to generalize to arbitrary world sizes and also helps reducing the input dimension to the neural net. However, agents need to have access to information about their goal location, which is often outside of the FOV. To this end, agents have access to a unit vector pointing towards their goal and Euclidean distance to their goal at all times (see Figure 2).

In the limited FOV, we separate the available information into different channels, to simplify the agents' learning task. Specifically, each agents' observation consists of binary matrices representing obstacles, positions of other agents, the agent's own goal location (if within the FOV), and the position of other observable agents' goals. When agents are close to the edges of the world, obstacles are added at all positions outside the world's boundaries.

B. Action Space

Agents take discrete actions in the grid world: moving one cell in one of the four cardinal directions or staying still. At each time step, certain actions may be illegal, such as moving into a wall or another agent. During training, actions are sampled only from valid actions and an additional loss function aids in learning this information. We experimentally observed that this approach enables more stable training, compared to giving negative rewards to agents for selecting invalid moves. Additionally, to combat convergence to oscillating policies, during training agents were prevented from moving back to the location they occupied at the last time step (agents can still stay still during multiple successive time steps). This was necessary to encourage exploration and learn effective policies (even with IL).

During testing of the learned policies, if an agent selects an invalid action, the agent instead stays still for that time step. In practice, agents very rarely select invalid actions once fully trained, showing that agents effectively learn the set of valid actions in each state.

C. Reward Structure

In this work, our reward function follows the same intuition that most reward functions for grid worlds use, where agents are punished for each step they are not resting on goal, leading to the optimal strategy of reaching their goal as quickly as possible. We penalize agents slightly more for staying still than for moving, which is necessary to encourage

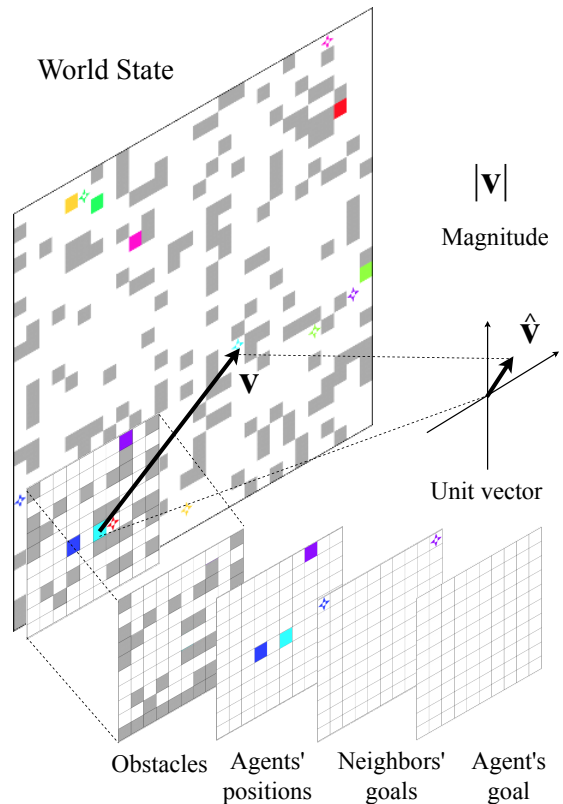


Fig. 2. Observation space of each agent (here, for the light blue agent). Agents are displayed as colored squares, their goals as similarly-colored stars, and obstacles as grey squares. Each agent only has access to a limited field of view (FOV) centered around its position, in which information are broken down into channels: positions of obstacles, of other agents nearby, goal position of these neighboring agents (projected at the boundary of the FOV if outside of the view), and position of one's goal if within the FOV. Note how the bottom row of the obstacle channel has been padded with obstacles, since these positions are outside of the world's boundaries. Agents also have access to a normalized vector pointing to their goal (often outside of their FOV), as well as its magnitude (distance to goal), as a natural way to let agents learn to select their general direction of travel.

exploration. Even though imitation assists in exploration, we found that removing this aspect of the reward function led to poor convergence, which we suspect is because the gradients from RL and IL conflict with each other. Though invalid moves (moving back to the previous cell, and moves resulting in obstacle collision) are filtered out of the action space during training as described in section III-B, because agents act sequentially in a random order, it is still possible for them to collide, e.g., when multiple agents choose to move to the same location at the same time step. Agent collisions result in a -2 reward. Agents receive a $+20$ bonus for finishing an episode, i.e., when all agents are on goal simultaneously. Our reward structure is summarized in Table I.

TABLE I
SIMPLE REWARD STRUCTURE.

Action	Reward
Move [N/E/S/W]	-0.3
Agent Collision	-2
No Movement (on/off goal)	0 / -0.5
Finish Episode	+20

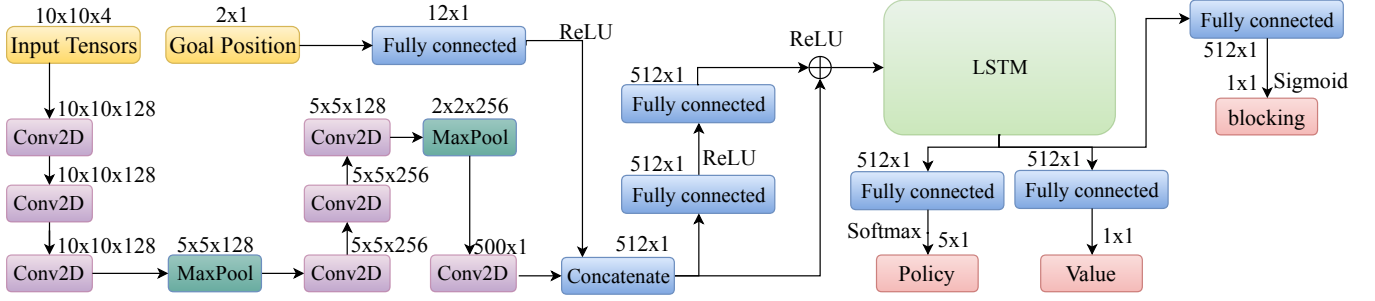


Fig. 3. The neural network consists of 6 convolution layers interleaved with maxpooling layers, followed by an LSTM.

D. Actor-Critic Network

This work relies on the asynchronous advantage actor-critic (A3C) algorithm [29], and extends our previous work in distributed learning for multiple agents in a shared environment [13], [14]. The agent’s policy is represented by a deep neural network with multiple outputs, one of them being the actual policy and the others only being used during training. We use the 6-layer convolutional network pictured in Fig. 3, taking inspiration from VGGnet [30], using several small 3×3 kernels between each max-pooling layer.

Specifically, the two inputs to the neural network – local observation and goal direction/distance – are pre-processed independently, before being concatenated half-way through the neural net. The four-channel matrices ($10 \times 10 \times 4$ tensor) representing the local observation of each agent are passed through two stages of three convolutions and maxpooling, followed by a last convolution layer. In parallel, the goal unit vector and magnitude are passed through one fully-connected layer. The concatenation of both of these pre-processed inputs is then passed through two fully-connected (fc) layers, which is finally fed into a long-short-term memory (LSTM) cell with output size 512. As often used to help convergence in deep networks, a residual shortcut [31] connects the output of the concatenation layer to the input layer of the LSTM. The output layers consist of the policy neurons with softmax activation, and a value output predicting the reward. We also added a feature layer connected to the LSTM [32], to train each agent to know whether it is blocking other agents from reaching their goal (detailed in Section IV-A.1).

During training, the policy, value and “blocking” outputs are updated in batch every $n = 256$ steps or when an episode finishes. As is common, the value is updated to match the total discounted return ($R_t = \sum_{i=0}^k \gamma^i r_{t+i}$) by minimizing:

$$L_V = \sum_{t=0}^n (V(o_t|\theta) - R_t)^2. \quad (1)$$

To update the policy we use an approximation of the advantage function by bootstrapping using the value function: $A(o_t, a_t|\theta) = \sum_{i=0}^{k-1} \gamma^i r_{t+i} + \gamma^k V(o_{t+k}|\theta) - V(o_t|\theta)$ (where k is bounded by the batch size). We also add an entropy term $H(\pi(o))$ to the policy loss, which has been shown to encourage exploration and discourage premature convergence [33] by penalizing a policy that always chooses the same actions. The policy loss reads

$$L_\pi = \sigma_H \cdot H(\pi(o)) - \sum_{t=0}^n \log(P(a_t|\pi, \theta, o)A(o_t, a_t|\theta)). \quad (2)$$

with a small entropy weight σ_H ($\sigma_H = 0.01$ in practice). We rely on two additional loss functions which help to guide and stabilize training. First, the blocking prediction output is updated by minimizing $L_{blocking}$, the log likelihood of predicting incorrectly. Second, we define the loss function L_{valid} minimizing the log likelihood of selecting an invalid action [13], as mentioned in section III-B.

IV. LEARNING

In this section, we detail our distributed framework to learn multi-agent path finding with implicit agent coordination. The reinforcement learning portion of our framework builds upon our previous works on distributed reinforcement learning for multiple agents in shared environments [13], [14]. In this work, we introduce an imitation learning module, where agents are presented with expert demonstrations.

A. Coordination Learning

One of the key challenges in training a decentralized policy is to encourage agents to act selflessly, even though it may be detrimental to their immediate maximization of reward. In particular, agents typically display undesirable selfish behavior when stopped on their goal while blocking other agents’ access to their own goals. A naive implementation of our previous work [13], where agents distributedly learn a fully selfish policy, collapses in dense environments with many narrow environmental features where the probability of blocking other agents is high. That is, agents simply learn to go as fast as possible to their goal, and then to never move from it even to let other agents access their own goal (despite the fact that this would end the episode early, which would result in higher rewards for all agents).

Many of the current methods surrounding this selfishness problem are invalidated by the size of the environments and the limited FOV of agents. Shared critics [25] have proven effective at multi-agent credit assignment. However, these methods are typically used when agents have nearly full information about the environment. In this highly decentralized scenario, assigning credit to agents may be confusing when they cannot observe the source of the penalty, for example when an agent cannot observe that a long hallway is a dead-end, yet the universal critic sharply decreases the value function. Another popular multi-agent training technique is applying joint rewards to agents in an attempt to help them realize the benefit of taking personal sacrifices to benefit the team [34], [14]. We briefly tried assigning

joint rewards to agents within the same observation space, however this produced no noticeable difference in behavior so we abandoned it in favor of the methods described below.

To successfully teach agents collaborative behavior, we relied on three methods: applying a penalty for inhibiting other agents’ movement (called the “blocking penalty”), using expert demonstrations during training, and tailoring the random environments during training to expose agents to more difficult cluttered scenarios. We emphasize that without all three methods, the learning process is either unstable (no learning) or converges to a worse policy than with all three, as is apparent in Fig. 5.

1) *Blocking Punishment*: We augment the reward function shown in Table I with a sharp penalty (-2 in practice) if an agent decides to stay on goal while blocking another from reaching its goal. The intuition behind this reward is to provide an incentive for agents to leave their goal, offsetting the (selfish) local maximum agents experience while resting on goal. Our definition of blocking includes cases where an agent isn’t just preventing any solution for another agent, but also cases where an agent lengthens the solution of another agent by a significantly (in practice, by 10 steps or more to match the size of agents’ FOV). This looser definition of blocking is necessary because of the agents’ small FOV. Although in larger worlds it is probable that an alternate route exists around a given agent, it is illogical to demand another path be found when coordination could lead to shorter paths, especially if the alternate route may lie outside the agent’s FOV (and therefore may be uncertain).

We use standard A^* to determine the length of an agent’s path to goal from its current position, and then that of its path when each other agent is removed from the world. For each other agent, if the second path is shorter than the current optimal one by more than 10 steps, that other agent is counted as blocking. The “blocking” output of the network is trained to predict when an agent is blocking others, to implicitly provide the agent with an “explanation” of the extra penalty it will incur.

2) *Combining IL and RL*: Second, combining imitation learning with reinforcement learning has been shown to lead to faster, more stable training as well as higher quality solutions in robot manipulation [35], [36]. Therefore, we let agents observe a demonstration of an optimal plan during a portion of the training episodes. Specifically, at the beginning of each episode, we randomly select whether the episode will involve reinforcement or imitation learning (see Fig. 4). Such demonstrations are generated dynamically by relying on the centralized planner ODrM* [3] (with $\epsilon = 2$). A trajectory of observations and actions $T \in (\mathcal{O} \times \mathcal{A})^n$ is obtained for each agent, and we minimize the behavior cloning loss:

$$L_{bc} = -\frac{1}{n} \sum_{(o,a) \in T} \log(P(a|\pi, o, \theta)). \quad (3)$$

Our implementation deviates from [35], [37] in that we combine off-policy behavior cloning with on-policy actor-critic learning, rather than with off-policy deep deterministic policy gradient. We explored this approach since we

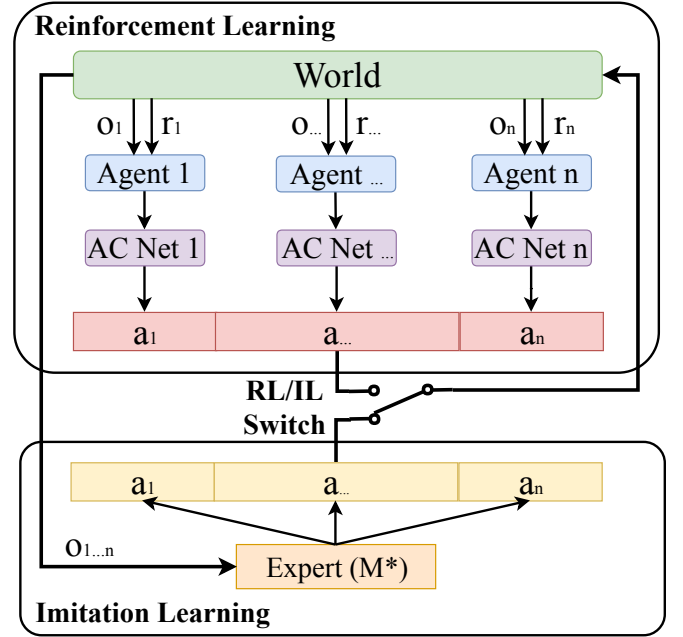


Fig. 4. Structure of our hybrid RL/IL approach. At the beginning of each episode, a random draw determines if the episode will be RL- or IL-based, and flips the corresponding “switch” (in the middle). For the RL part of the learning, at each time step, each agent $(1, \dots, n)$ draws its observation o_i and previous reward r_i from the world (learning environment), and uses the observation to select an action a_i via its own copy of the neural net. Actions are executed sequentially in a random order. Since agents often push and pull weights from a common, shared neural net, agents ultimately all share the same weights in their individual nets. For the IL-based learning, an expert centralized algorithm coordinates all agents during the episode, whose behavior agents also learn to clone (coordination learning between agents).

can cheaply generate expert demonstrations online at the beginning of a new training episode, as opposed to other works where learning agents only have access to a finite set of pre-recorded expert trajectories; our experiments show it produces very good results.

Leveraging demonstrations is a necessary component of our system: without it learning progresses far slower and converges to a significantly worse solution. However, we experimented with various IL proportions (10 – 50% by increments of 10%), and observed that the IL/RL ratio does not seem to affect the performance of the trained policy by much. Finally, though we could use dynamic methods such as DAGGER [38] or confident inference [39] because of the availability of a real-time planner, we chose to use behavior cloning because of its simplicity and ease of implementation. It is unclear whether using such methods would lead to a performance increase, and will be the subject of future works.

3) *Environment Sampling*: Finally, we found that uniformly sampling the size and densities of worlds did not expose agents to enough situations in which coordination was necessary because of the relative sparsity of agent-agent interactions. Instead, during training, we randomize both the size and obstacle density of worlds at the beginning of each episode. We sample both size and density from a distribution favoring smaller and denser environments, forcing agents to learn coordination since they experience crowded environments more often.

B. Training Details

1) *Environment*: The size of square environments was randomly selected at the beginning of each episode to be either 10, 40, or 70, with a probability distribution making 10-size worlds twice as likely. The obstacle density was randomly selected from a triangular distribution between 0 and 50%, with the peak centered at 33%. Placement of obstacles, agents, and goals was uniformly random across the environment, with the caveat that each agent had to be able to reach its goal. That is, each agent must initially be placed in the same connected region as their goal, disregarding other agents in the same region. Technically, it is possible that agents train on impossible environments (e.g., two agents spawned in the same narrow connected region, each on the other's goal), though highly unlikely. Because agents' actions are enacted sequentially in a random order, race conditions are resolved at random.

2) *Parameters*: We use a discount factor (γ) of 0.95, an episode length of 256, and a batch size of 128 so that up to two gradient updates are performed each episode per agent. The probability of observing a demonstration is 50% per episode. We use the Nadam optimizer [40], with a learning rate beginning at $2 \cdot 10^{-5}$ and decaying proportionally to the inverse square root of episode count. We train in 3 independent environments with 8 agents each, synchronizing agents in the same environment at the beginning of each step and allowing them to act in parallel. Training was performed at the Pittsburgh Supercomputing Center (PSC) [41], on 7 cores of a Intel Xeon E5-2695 and one NVIDIA K80 GPU, and lasted around 20 days. The full code used to train agents is available at <https://goo.gl/T627XD>.

V. RESULTS

In this section, we present the results of an extensive set of simulations we performed to compare PRIMAL against different state-of-the-art MAPF algorithms in grid worlds. These tests are performed in environments with varying obstacle densities and grid sizes. Finally, we present experimental results in a scenario featuring both physical and simulation robots planning paths online in an indoor factory mockup.

A. Comparison with Other MAPF Planners

For our systematic experiments, we selected CBS [19] as our optimal, centralized planner, ODrM* [3] as a suboptimal, centralized option (with inflation factors $\epsilon = 1.5$ and $\epsilon = 10$), as well as ORCA [5] as a fully-decoupled velocity planner. Note that all the other planners have access to the whole state of the system, whereas PRIMAL assumes each agent only has partial observability of the system. World sizes were systematically varied between $\{10, 20, 40, 80, 160\}$, densities between $\{0, 0.1, 0.2, 0.3\}$ and agent numbers between $\{4, 8, \dots, 512\}$. We placed no more than 32 agents in 10-size worlds, and no more than 128 in 20-size worlds.

In our tests, we compared the success rates of the different planners, that is whether or not they can complete a given problem within a given amount of physical time or time steps. For CBS and ODrM*, we used a timeout of 300s

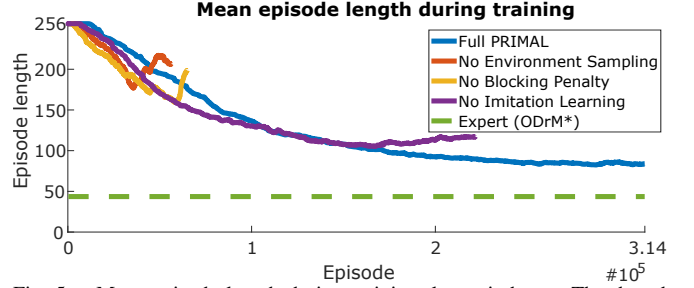


Fig. 5. Mean episode length during training, lower is better. The dotted line shows the reference, measured from the expert ODrM* algorithm. When we remove either environment sampling, blocking penalties, or expert demonstrations from our approach, the policy converges to a worse solution.

(CBS), and 60s respectively, to match previous results [3]. Note that we divided the timeout by 5 for ODrM* since we were using the C++ version of the code which was experimentally measured to be about 5 times faster as the previously used python implementation. For ORCA, we use a timeout of 60s, but also stop the code early if all agents are in a deadlock (measured as all agents being stuck for more than 120s in simulation time, which is about 10s in physical time). Finally, for PRIMAL, we let the agents plan individual paths for up to 256 time steps for 10- to 40-size worlds, 384 steps for 80-size worlds and 512 steps for 160-size worlds. Tests for the conventional planners were carried out on a single desktop computer, equipped with an AMD Threadripper 2990WX with 64 logical cores clocked at 4Ghz and 64Gb of RAM. Tests for PRIMAL were partially run on the same computer, which is also equipped with 3 GPUs (NVIDIA Titan V, GTX 1080Ti and 1070Ti), as well as on a simple desktop with an Intel i7-7700K, 16Gb RAM and a NVIDIA GTX 1070.

Based on our results, a first general observation is that our approach performs extremely well in low obstacle densities, where agents can easily go around each other, but is easily outperformed in dense environments, where joint actions seem necessary for agents to reach their goal (which sometimes require drastic path changes). Similarly, but with significantly worse performances, ORCA cannot protect against deadlocks and performs very poorly in most scenarios involving more than 16 agents and any obstacles, due to its fully-decoupled, reactive nature. Second, we notice that, since our training involves worlds of varying sizes but a constant team size, agents are inherently exposed to a small variability in agent density within their field of view. In our results, we observed that agents perform more poorly as the number of neighboring agents increases in their FOV (small worlds, large teams), an effect we believe could be corrected by varying the team sizes during training. This will be investigated in future works; however, we expect traditional planners to generally outperform our approach in small worlds (10-20 size), even with larger teams. Third, we noticed that the paths generated by PRIMAL were sometimes more than twice as long as the other planners'. However, other planners allow moves that the agents cannot take in our definition of the MAPF problem: agents can follow each

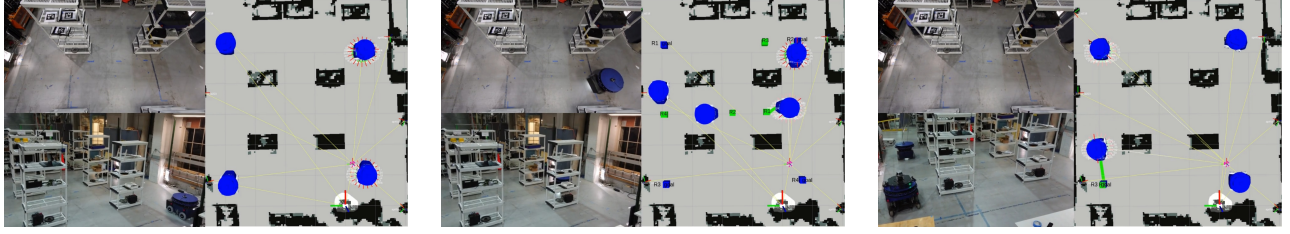


Fig. 6. Successive frames of the physical and simulated robots exchanging positions in the factory mockup.

other with no empty space between them, can swap around (similar to a runabout), etc. [3], which leads to shorter paths. Additionally, visual inspection of the cases where PRIMAL generates longer paths shows that most agents move to their goals efficiently, except for a few laggards. Finally, since agents were never exposed to worlds larger than 70×70 during training, they seem to perform extremely poorly in larger worlds during testing (≥ 80 -sized). However, by capping the goal distance in the agents' state, PRIMAL's success rate in larger worlds can be drastically improved. In the results presented here for 80- and 160-sized worlds, the distance to goals is capped at 75 (empirically set) in the agents' state. Example video results of near-optimal and severely sub-optimal plans for PRIMAL in various environments are available at <https://goo.gl/T627XD>.

Due to space constraints, we choose to discuss the three main scenarios shown in Fig. 7: a case where PRIMAL strongly outperforms all other planners, one where PRIMAL slightly outperforms them, and a case where PRIMAL particularly struggles. The complete set of results (for all agents team sizes, obstacles densities and world sizes) can be found at <https://goo.gl/APktNk>, and also details the different paths lengths generated by the different planners as well as planning times. First, in a large world with no obstacle (160×160), centralized planners especially struggle, since the joint configuration space quickly grows to encompass all agents, making planning for more than 100 agents very difficult. There, PRIMAL can easily deal with teams up to 1024 agents, with a near-perfect success rate. Second, in a medium-sized world with low obstacle density, the centralized planners can easily plan for a few hundred agents. PRIMAL's success rate starts decreasing earlier than the other planners, but can still handle above 60% of cases with 512 agents, whereas all other planners are out of the competition. Third, in a smaller world, very densely populated with obstacle, all planners can only handle up to 64 agents, but PRIMAL starts struggling past 8 agents, whereas ODrM* can confidently handle up to 64 agents. However, note that even when PRIMAL cannot finish a full problem, it usually manages to bring many agents to their goal quickly, with only a few failing to reach their goals. At this point, a conventional planner could be used to complete the problem, which has usually become a simple problem for a graph-based solver since most agents should remain motionless at their goals. Future work will investigate the combination of PRIMAL with a complete planner, to leverage the fast, decentralized planning of PRIMAL while guaranteeing completeness.

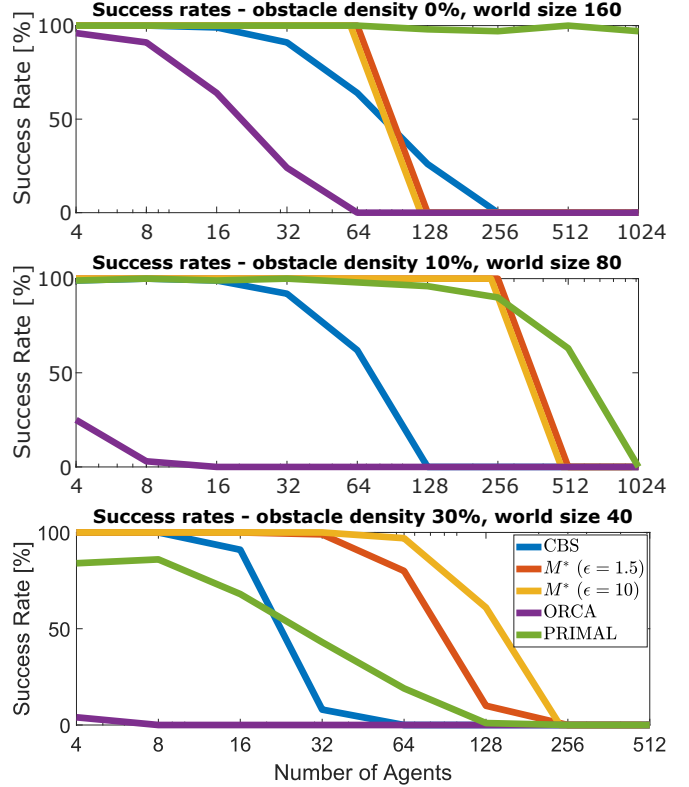


Fig. 7. Success rates of the different planners in the three scenarios on which we chose to focus. Note how PRIMAL outperforms all planners in the top example (no obstacles), slightly outperforms the others in low-density worlds, and is strongly outperformed in dense obstacles.

B. Experimental Validation

We further implemented PRIMAL on a small fleet of autonomous ground vehicles (AGVs) [42] evolving in an indoor factory mockup. In this hybrid system, two physical robots evolve alongside two (then, half-way through the experiment, three) simulated ones. Physical robots have access to the position of simulated robots, as they plan their next action online using our decentralized approach. PRIMAL shows clear online capabilities, as planning time per step and per agent is well below 0.1s on a standard GPU (well below 0.2s on CPU). Fig. 6 shows a series of frames during a planning instance, where robots are commanded to exchange their positions. The full video is available at <https://goo.gl/T627XD>.

VI. CONCLUSION

In this paper, we presented PRIMAL, a new approach to multi-agent path finding, which relies on combining distributed reinforcement learning and imitation learning from

a centralized expert algorithm. Through an extensive set of tests, we show how PRIMAL naturally scales to various team sizes, world sizes and obstacle densities, despite only giving agents access to local information about the world. In low obstacle-density environments, we further show how PRIMAL exhibits on-par performances, and even outperform state-of-the-art MAPF planners in certain cases, even though these have access to the whole state of the system. Finally, we presented an example where we deployed PRIMAL on physical and simulated robots in a factory mockup scenario, showing how robots can benefit from our online, local-information-based, decentralized MAPF approach.

Future works will focus on adapting our training procedure for factory-like environments, where obstacle density may be overall low to medium but where parts of the environment are very sparse and other highly-structured (corridors, aisles, etc.). We also believe that extending our approach to receding-horizon planning, where agents plan ahead for several actions, may help improve the performances of PRIMAL by teaching agents to explicitly coordinate their paths.

ACKNOWLEDGMENTS

Guillaume Sartoretti would like to thank Manufacturing Future Initiatives (MFI) for funding his work on this project. Justin Kerr would like to thank the National Science Foundation for funding his work on this project as part of the 2018 CMU SURF program. The research at the University of Southern California was supported by the National Science Foundation (NSF) under grant number 1409987. This work used the Bridges system, which is supported by NSF award number ACI-1445606, at the Pittsburgh Supercomputing Center (PSC) [41].

REFERENCES

- [1] M. Rubenstein, A. Cornejo, and R. Nagpal, "Programmable self-assembly in a thousand-robot swarm," *Science*, vol. 345, no. 6198, pp. 795–799, 2014.
- [2] A. Howard, L. E. Parker, and G. S. Sukhatme, "Experiments with a Large Heterogeneous Mobile Robot Team: Exploration, Mapping, Deployment and Detection," *The International Journal of Robotics Research*, vol. 25, no. 5-6, pp. 431–447, 2006.
- [3] G. Wagner and H. Choset, "Subdimensional expansion for multirobot path planning," *Artificial Intelligence*, vol. 219, pp. 1–24, 2015.
- [4] M. Barer, G. Sharon, R. Stern, and A. Felner, "Suboptimal Variants of the Conflict-Based Search Algorithm for the Multi-Agent Pathfinding Problem," in *Proceedings of SoCS*, 2014.
- [5] J. Van Den Berg, S. J. Guy, M. Lin, and D. Manocha, "Reciprocal n-body collision avoidance," in *Robotics research*, 2011, pp. 3–19.
- [6] R. Cui, B. Gao, and J. Guo, "Pareto-optimal coordination of multiple robots with safety guarantees," *Autonomous Robots*, vol. 32, no. 3, pp. 189–205, Dec. 2011.
- [7] J. L. Baxter, E. Burke, J. M. Garibaldi, and M. Norman, "Multi-robot search and rescue: A potential field based approach," in *Autonomous robots and agents*. Springer, 2007, pp. 9–16.
- [8] H. Balakrishnan and Y. Jung, "A framework for coordinated surface operations planning at Dallas-fort Worth international airport," in *AIAA Guidance, Navigation, and Control Conf.*, vol. 3, 2007, pp. 2382–2400.
- [9] M. Bonert, L. Shu, and B. Benhabib, "Motion planning for multi-robot assembly systems," *International Journal of Computer Integrated Manufacturing*, vol. 13, no. 4, pp. 301–310, 2000.
- [10] K.-H. C. Wang and A. Botea, "MAPF: a scalable multi-agent path planning algorithm with tractability and completeness guarantees," *Journal of Artificial Intelligence Research*, vol. 42, pp. 55–90, 2011.
- [11] Y. F. Chen, M. Liu, M. Everett, and J. P. How, "Decentralized non-communicating multiagent collision avoidance with deep reinforcement learning," in *Proceedings of ICRA*, 2017, pp. 285–292.
- [12] R. S. Sutton and A. G. Barto, "Reinforcement learning: An introduction. 1998," *A Bradford Book*, 1998.
- [13] G. Sartoretti, Y. Wu, W. Paivine, T. K. S. Kumar, S. Koenig, and H. Choset, "Distributed Reinforcement Learning for Multi-Robot Decentralized Collective Construction," in *Accepted to DARS*, 2018.
- [14] G. Sartoretti, Y. Shi, W. Paivine, M. Travers, and H. Choset, "Distributed Learning for the Decentralized Control of Articulated Mobile Robots," in *Proceedings of ICRA*, 2018.
- [15] S. Leroy, J.-P. Laumond, and T. Siméon, "Multiple Path Coordination for Mobile Robots: A Geometric Algorithm," in *Proceedings of the IJCAI*, 1999, pp. 1118–1123.
- [16] M. Cáp, P. Novák, M. Selecký, J. Faigl, and J. Vokínek, "Asynchronous Decentralized Prioritized Planning for Coordination in Multi-Robot System," in *IROS*, 2013, pp. 3822–3829.
- [17] M. Erdmann and T. Lozano-Perez, "On multiple moving objects," *Algorithmica*, vol. 2, no. 1, pp. 477–521, 1987.
- [18] G. Sanchez and J. Latombe, "Using a PRM planner to compare centralized and decoupled planning for multi-robot systems," in *Proceedings of the IEEE International Conference on Robotics and Automation*, vol. 2, Washington D.C., USA, 2002, pp. 2112–2119.
- [19] G. Sharon, R. Stern, A. Felner, and N. Sturtevant, "Conflict-based search for optimal multi-agent path finding," in *Proceedings of the AAAI Conference on Artificial Intelligence*, 2012.
- [20] C. Ferner, G. Wagner, and H. Choset, "ODrM* optimal multirobot path planning in low dimensional search spaces," in *Proceedings of ICRA*. IEEE, 2013, pp. 3854–3859.
- [21] T. Standley, "Finding Optimal Solutions to Cooperative Pathfinding Problems," in *Proceedings of AAAI Conference on Artificial Intelligence*, 2010, pp. 173–178.
- [22] L. Buoni, R. Babuška, B. De Schutter, D. Srinivasan, L. C. Jain, L. Buoni, R. Babuška, and B. De Schutter, "Multi-agent reinforcement learning: An overview," *of Studies in Computational Intelligence*, vol. 310, pp. 183–221, 2010.
- [23] J. K. Gupta, M. Egorov, and M. Kochenderfer, "Cooperative multi-agent control using deep reinforcement learning," in *Proceedings of AAMAS*. Springer, 2017, pp. 66–83.
- [24] R. Lowe, Y. Wu, A. Tamar, J. Harb, O. P. Abbeel, and I. Mordatch, "Multi-agent actor-critic for mixed cooperative-competitive environments," in *Advances in NIPS*, 2017, pp. 6382–6393.
- [25] J. Foerster, G. Farquhar, T. Afouras, N. Nardelli, and S. Whiteson, "Counterfactual multi-agent policy gradients," *arXiv preprint 1705.08926*, 2017.
- [26] J. Foerster, I. A. Assael, N. de Freitas, and S. Whiteson, "Learning to communicate with deep multi-agent reinforcement learning," in *Advances in NIPS*, 2016, pp. 2137–2145.
- [27] F. S. Melo and M. Veloso, "Heuristic Planning for Decentralized MDPs with Sparse Interactions," in *Distributed Autonomous Robotic Systems*. Springer, 2013, pp. 329–343.
- [28] T. Schaul, J. Quan, I. Antonoglou, and D. Silver, "Prioritized experience replay," *arXiv preprint 1511.05952*, 2015.
- [29] V. Mnih, A. P. Badia, M. Mirza, A. Graves, T. Lillicrap, T. Harley, D. Silver, and K. Kavukcuoglu, "Asynchronous methods for deep reinforcement learning," in *ICML*, 2016, pp. 1928–1937.
- [30] K. Simonyan and A. Zisserman, "Very deep convolutional networks for large-scale image recognition," *arXiv preprint 1409.1556*, 2014.
- [31] K. He, X. Zhang, S. Ren, and J. Sun, "Deep Residual Learning for Image Recognition," in *The IEEE Conference on Computer Vision and Pattern Recognition (CVPR)*, June 2016.
- [32] G. Lample and D. S. Chaplot, "Playing FPS Games with Deep Reinforcement Learning," in *AAAI*, 2017, pp. 2140–2146.
- [33] M. Babaeizadeh, I. Frosio, S. Tyree, J. Clemons, and J. Kautz, "Reinforcement learning through asynchronous advantage actor-critic on a GPU," in *Proceedings of ICLR*, 2017.
- [34] P. Ying and L. Dehua, "Improvement with joint rewards on multi-agent cooperative reinforcement learning," in *Proceedings of CASCON*, vol. 1. IEEE, 2008, pp. 536–539.
- [35] A. Nair, B. McGrew, M. Andrychowicz, W. Zaremba, and P. Abbeel, "Overcoming exploration in reinforcement learning with demonstrations," *arXiv preprint 1709.10089*, 2017.
- [36] A. Rajeswaran, V. Kumar, A. Gupta, J. Schulman, E. Todorov, and S. Levine, "Learning complex dexterous manipulation with deep reinforcement learning and demonstrations," *CoRR*, vol. 1709.10087, 2017.

- [37] M. Vecerík, T. Hester, J. Scholz, F. Wang, O. Pietquin, B. Piot, N. Heess, T. Rothörl, T. Lampe, and M. A. Riedmiller, "Leveraging demonstrations for deep reinforcement learning on robotics problems with sparse rewards," *CoRR*, *abs/1707.08817*, 2017.
- [38] S. Ross, G. Gordon, and D. Bagnell, "A reduction of imitation learning and structured prediction to no-regret online learning," in *Proceedings of ICAIS*, 2011, pp. 627–635.
- [39] S. Chernova and M. Veloso, "Confidence-based policy learning from demonstration using gaussian mixture models," in *Proceedings of ACM*, 2007, p. 233.
- [40] T. Dozat, "Incorporating nesterov momentum into Adam," 2016.
- [41] N. A. Nystrom, M. J. Levine, R. Z. Roskies, and J. R. Scott, "Bridges: A Uniquely Flexible HPC Resource for New Communities and Data Analytics," in *Proceedings of the XSEDE Conf.*, 2015, pp. 30:1–30:8.
- [42] D. Bourne, H. Choset, H. Hu, G. Kantor, C. Niessl, Z. Rubinstein, R. Simmons, and S. Smith, "Mobile manufacturing of large structures," in *Proceedings of ICRA*. IEEE, 2015, pp. 1565–1572.